Relationship between Polarity of Template Hydrogel and Nanoporous Structure Replicated in Sol–Gel-Derived Silica Matrix

K. Kurumada, A. Suzuki, S. Baba, E. Otsuka

School of Environment and Information Sciences, Yokohama National University, Yokohama 240-8501, Japan

Received 18 February 2009; accepted 11 July 2009
DOI 10.1002/app.31095
Published online 19 August 2009 in Wiley InterScience (www.interscience.wiley.com).

ABSTRACT: We replicated the nanoscopic network structure of acrylamide series hydrogels in silica matrix. In the replication, the mutual affinity of the template polymeric species to sol–gel-derived silica matrix significantly affects the replicated porous structure formed in the silica matrix. In this work, we intended to fabricate nanoscopic replicas of hydrogels of acrylamides with various hydrophobic end groups. First, the alcoxy silane, tetraethylorthosilicate (TEOS) was hydrolyzed with the template hydrogel. Subsequently, the nanoporous silica solid structure was obtained by removing the hydrogel by calcination in air at 600°C. The nanoscopic structure of those replicas was estimated by transmission electron microscopy (TEM) and nitrogen adsorption/desorption at 77 K. Basically, the nanoscopic replication was possible using the examined hydrogels of polyacrylamides. As the template hydrogel became more nonpolar, the size of the nanopores in the silica replica increased. Thus, the contrast in the polarity between the template hydrogel and silica matrix leads to the enhanced driving force for the mutual segregation or phase separation to occur. The replicated nanoporous structure is considered as a type of a transient structure arrested on the way to the completion of the phase separation of the template polymeric species from the silica matrix. Therefore, the larger contract in the polarity between the structure directing hydrogel and solid matrix lead to the formation of the larger nanopores because of the enhancement in the driving force toward the segregation. © 2009 Wiley Periodicals, Inc. J Appl Polym Sci 114: 4085–4090, 2009

Key words: hydrogels; networks; silica; nanoscopic replication; acrylamide

INTRODUCTION

A hydrogel generally has a nanoscopic mesh-like structure. Such a topologically constrained microscopic structure is the physical root of the prominent properties of hydrogels like macroscopically tangible elasticity. The nanoscopic mesh-like geometry is a quite universal structure spontaneously formed in a swollen state of a hydrogel. For this reason, the technique to replicate those nanoscopic solid matters attracts interest from the viewpoints of both science and engineering. Particularly, the potential ability of hydrogel to work as nanoscopic template for fabrication of nanoporous structure is worth considering from the technical viewpoints of nanofabrications. There have been many proposed approaches for fabricating nanoporous materials. It is often the case that the technical complications in the procedures for those fabrications are the problems to be solved in the practical standpoints. Because the nanoscopic network structure formed in a hydrogel is spontaneously formed, it can work as a practical and technical solution to the aforementioned problem.

However, the replication of the nanoscopic mesh of the hydrogel in a fully swollen state is technically quite hard. In cases of the majority of previous studies, hydrogels were used as the templates in which microparticles were formed.[1–16] The microstructure in the hydrogel was reported to trigger or promote anisotropic growth of microparticles formed in the hydrogel.[1,3,9,14] Although these studies took advantage of the structural features of the topologically constrained microstructure of the hydrogel, they did not include the concept of fabricating the nanoscopic replica of the hydrogel. Other major cases of using hydrogels as media for formation of solid materials are found in the biomimetic methods to fabricate biocompatible materials.[17–23] In these approaches, the elastic hydrogel was considered as a pseudo-biological tissue in which various biocompatible solids are spontaneously generated. Nevertheless, in those works, whether the nanoscopic mesh-like structure of the template hydrogel could be reflected on the micro- or mesostructure of the obtained biocompatible materials was not the central issue.

We focused our attention on the viable method to replicate the nanoscopic mesh in the sol–gel-derived silica matrix.[24–26] The technological point of this

Correspondence to: K. Kurumada (kurumada@ynu.ac.jp).
Contract grant sponsor: Hitachi Chemical Co. Ltd.

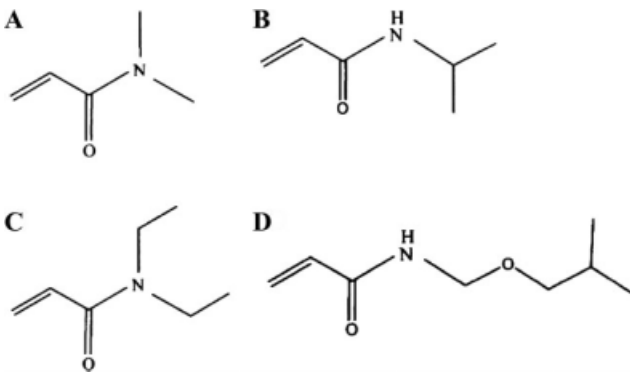

Figure 1 Chemical structural formulae of monomers of the four hydrogel species used in this work. (A) *N,N′*-dimethylacrylamide (DMAM), (B) *N*-isopropylacrylamide (NIPAM), (C) *N,N′*-diethylacrylamide (DEAM), (D) *N*-isobutoxyacrylamide (IBMAM).

method is a proposal of an extension of the approaches to "nanofabrocation". In these works, the polymerization and crosslinking were simultaneously caused in the solidifying sol–gel-derived silica matrix. The micro- and mesoscopic morphology of the hydrogel was obtained by eliminating the hydrogel by the oxidative calcination in air at 600°C. The increase in the volume fraction of the template hydrogel lead to the enhanced size of the nanopores in the replica. As a natural extension of this idea, we can consider the variation in the polarity of the template hydrogel as an influential factor on the resultant porous structure of the silica replica. Thus, we intended to replicate the nanoscopic mesh-like structure of acrylamide (AAM) series hydrogels with the hydrophobic end groups varied in their length as shown in Figure 1. Based on the experimentally clarified structural features of the nanopores in the silica replicas, the correlation between the polarity of the template hydrogel and mode of the replication into the silica matrix will be discussed.

EXPERIMENTAL

Materials

N,N′-dimethylacrylamide (DMAM) (98%), *N,N′*-diethylacrylamide (DEAM) (98%), *N*-isobutoxyacrylamide (IBMAM) (95%), *N,N′*-methylene(bisacrilamide) (BIS) (98%), *N,N,N,N*-tetramethylethylenediamide (TEMED) (95%), ammonium peroxodisulfate (APS) (98%), and 1*M* hydrochloric acid (HCl) were purchased from Wako Pure Chemical. *N*-isopropylacrylamide (NIPAM) (98%) was purchased from Kojin Chemical. Tetraethylorthosilicate (TEOS) (95%) was purchased from Tama Chemical. All of these chemicals were used as provided without further purification. The water used for the sample preparation was purified by ion exchange followed by distillation.

Preparation of samples

The silica preform sol was prepared by hydrolyzing TEOS (20.8 g, 0.10 mol) with water (18.0 g, 1.0 mol) and 1.0*M* HCl (0.10 g) under vigorous stirring using a magnetic stirrer. Here, the limiting component was TEOS, which was to yield 6.0 g of silica. Here, the molar ratio of the added water for the hydrolysis to TEOS was 10. Because the stoichiometric molar ratio of water TEOS is 4 for the complete hydrolysis, water was excessively contained in the reaction solution. Therefore, the expected molar number of silica to be formed by the aforementioned process was 1.0×10^{-1}. The samples were prepared at various weight ratios (ε) of the template polymeric species to silica in the range of $0.5 \leq \varepsilon \leq 5$. For the weight ratio ε, the preform solution of the hydrogel was prepared as follows: 6 ε g, 9.35×10^{-2} ε g, and 1.00×10^{-1} ε g of each monomer, BIS, and TEMED, respectively, were mixed and stirred until a clear solution was obtained. Here, 24 ε g of water was added only in the case of NIPAM for the dissolution of the powdery NIPAM monomer. Figure 2 presents the preparation scheme of the sample. The hydrolysis of TEOS to prepare the silica sol was continued for an hour. Just after beginning the stirring, TEOS separated from the aqueous phase because of its hydrophobicity by the bulky four ethyl groups. Once the hydrolysis started, the mixture turns to a uniphasal clear solution because of the formation of ethanol by the hydrolysis of TEOS. Subsequently, the hydrolytic reaction drastically accelerated because of the enhancement in the frequency of the molecular contacts between TEOS and water. During the 1 h of the hydrolysis, tangible exothermic behavior was observed between 20 and 30 min of the lapse of the time after beginning the hydrolysis. After 1 h for the hydrolysis of TEOS, the preform solution of the template hydrogel kept refrigerated at 5°C was added followed by quick addition and mixing of 1.0 g of 4 wt % APS aqueous solution to trigger the polymerization and crosslinking. Then, the whole preform was kept still for 6 h at room temperature ($\sim$ 20°C). The gellation was observed during this aging period. After this, the obtained wet hybridized gel of silica and AAM series hydrogel was dried for 48 h at 80°C to complete the polymerization. Finally, the template hydrogel was eliminated by calcination in air for 5 h at 600°C.

Observations and measurements

The transmission electron microscopy (TEM) observations were carried out at 175 or 200 kV of the

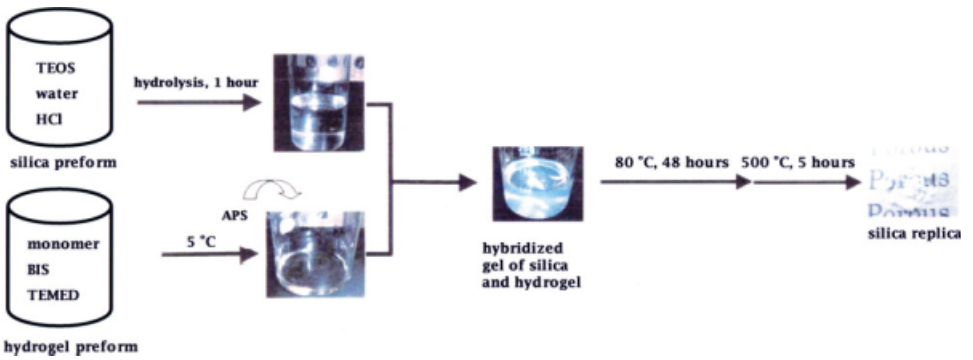

Figure 2 Scheme of the sample preparation. The silica replica of the hydrogel was prepared from the preform solution of silica and the template hydrogel. The hybridized gel was followed by a drying and calcination process in order to eliminate the template hydrogel. [Color figure can be viewed in the online issue, which is available at www.interscience.wiley.com.]

acceleration voltage (HITACH H - 800, Hitachi, Japan). The sample was carefully ground, sparsely dispersed in ethanol, and placed on a microgrid by dripping a drop of the above dispersion. The nitrogen adsorption/desorption measurements were carried out at 77 K using Belsorp Mini (Nippon Bell, Japan). The saturated adsorption volume (maximum adsorbed volume) was obtained at the relative pressure $P/P_0 = 0.9814$, where P and P_0 denote the equilibrium and ambient pressure, respectively. The total volume of the nanopore in the covered range by the nitrogen adsorption/desorption was evaluated using the values 808 kg m^{-3} of the bulk density of liquid nitrogen. The pore size distribution was calculated by the Barrett–Joyner–Halenda (BJH) method.[27]

RESULTS AND DISCUSSION

Outside appearance

Figure 3 presents the outside appearance of the hybridized wet gels and silica replicas after the elimination of the template hydrogel. In the cases where DMAM and NIPAM were used as the template hydrogel, the samples were optically transparent both before and after the elimination of the template hydrogel. In contrast, the use of DEAM and IBMAM, which are relatively nonpolar templates among the four species, resulted in the opaque appearance both before and after the elimination. Here, the transparency and opacity are considered as rough indications of the extent of the inhomogeneity of the structure. The transparency is to be linked with the relatively homogeneous structure and vice versa. The scale of the inhomogeneity in the case of the transparent appearance should be below 102 nm in the order of magnitude. On the other hand, the opaque samples are likely to have structural inhomogeneity over the above spatial scale. Thus, it can be claimed that, at least, the opaque samples had nonnegligibly larger structural inhomogeneities than the transparent ones. Therefore, a more hydrophilic template hydrogel forms a more homogeneous composite state with the silica matrix. The opacity in cases of DEAM and IBMAM shows that these two relatively hydrophobic template hydrogels induce the mutual segregation from

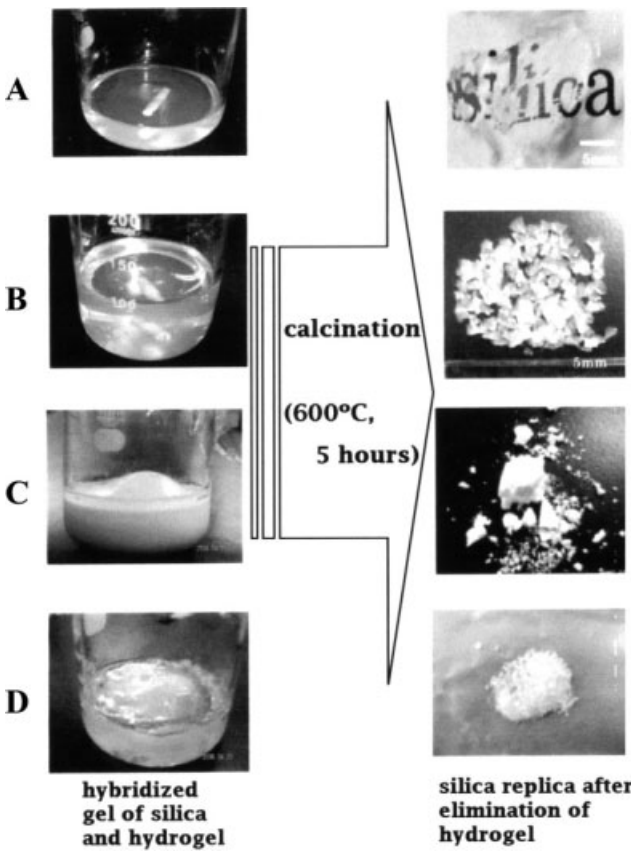

Figure 3 Outer appearance of the hybridized gel of silica and the template hydrogel (left) and the silica replica after the elimination of the template hydrogel (right). (A) *N*,*N*′-dimethylacrylamide (DMAM), (B) *N*-isopropylacrylamide (NIPAM), (C) *N*,*N*′-diethylacrylamide (DEAM), (D) *N*-isobutoxyacrylamide (IBMAM). The weight ratio ε of the hydrogel to silica was set at unity.

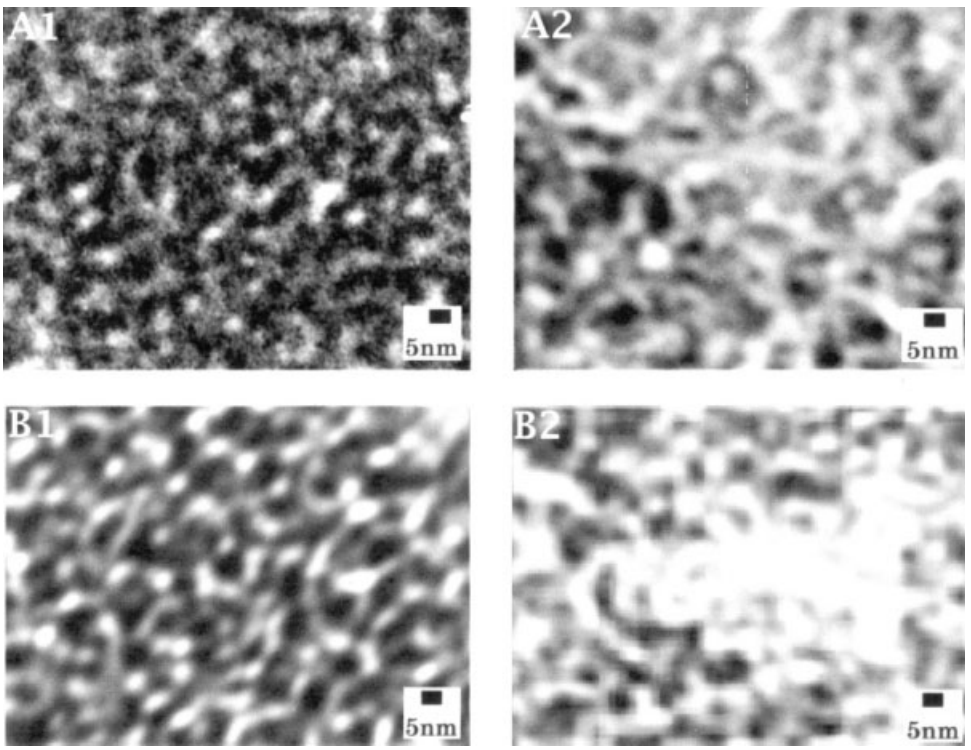

Figure 4 Transmission electron microscopy images of the silica replicas prepared with DMAM (A1 and A2) and NIPAM (B1 and B2). (A1) DMAM, $\varepsilon = 1$. (A2) DMAM, $\varepsilon = 3$. (B1) NIPAM, $\varepsilon = 1$. (B2) NIPAM, $\varepsilon = 3$.

the solidifying silica matrix over the spatial scale of the wavelength of the visible light. On the contrary, the spatial scale of the segregation was small enough to retain the optical transparency when the relatively polar template hydrogel species, DMAM and NIPAM, were used. These results indicate that spatial scale of the inhomogeneity formed in the wet hybridized state is noticeably influential on the structure of the silica replica after the elimination of the template hydrogel. That is, the finer structure of the silica replica tends to be formed from the more homogeneously hybridized composite state of the silica matrix and template hydrogel.

TEM observations

Figure 4 presents the TEM images of the silica replicas obtained using DMAM and NIPAM. The lighter parts correspond to the pores or voids in the sample. "Worm-like" nanopores are seen ubiquitously distributed in the sample. Such a nanoscopic geometry is much like those seen in our previous works, where we used only NIPAM as the template hydrogel.[25–27] A comparison between the two cases of DEAM and NIPAM at $\varepsilon = 3$ suggests that the NIPAM template hydrogel has a greater tendency to segregate from the solidifying silica matrix than DEAM. The voids of the scale of 101 nm seen at $\varepsilon = 3$ of NIPAM are considered as the transient structure toward the phase separation arrested during the progress of the solidification of the silica matrix. Within the range of a qualitative illustration, NIPAM has a greater driving force for the phase separation. As a result of that, the segregation (phase separation, evolution of the domains) further proceeds in the case of NIPAM than that of DEAM.

Size distribution of nanopores

Figure 5 shows the BJH size distribution of the nanopores of the silica replicas obtained using the four sorts of the template hydrogels. In all the cases, the radius of the nanopore increased with the weight ratio ε of the template hydrogel. It needs to be noted that the extent of the above increase in the size of the nanopore enhanced in order of the nonpolarity of the template hydrogel from DMAM to IBMAM. This result is consistent with the aforementioned speculation that the less polar moiety exhibits a greater tendency of the segregation in the silica matrix leading to the larger nanopores in the resultant replicated structure of the silica matrix. In an overall comparison among the four cases of these template hydrogels, the change in the size distribution was the most prominent between the cases of NIPAM and DEAM. This relatively abrupt change in the size distribution of the nanopore appears to overlap the change in the outside appearance shown in Figure 3.

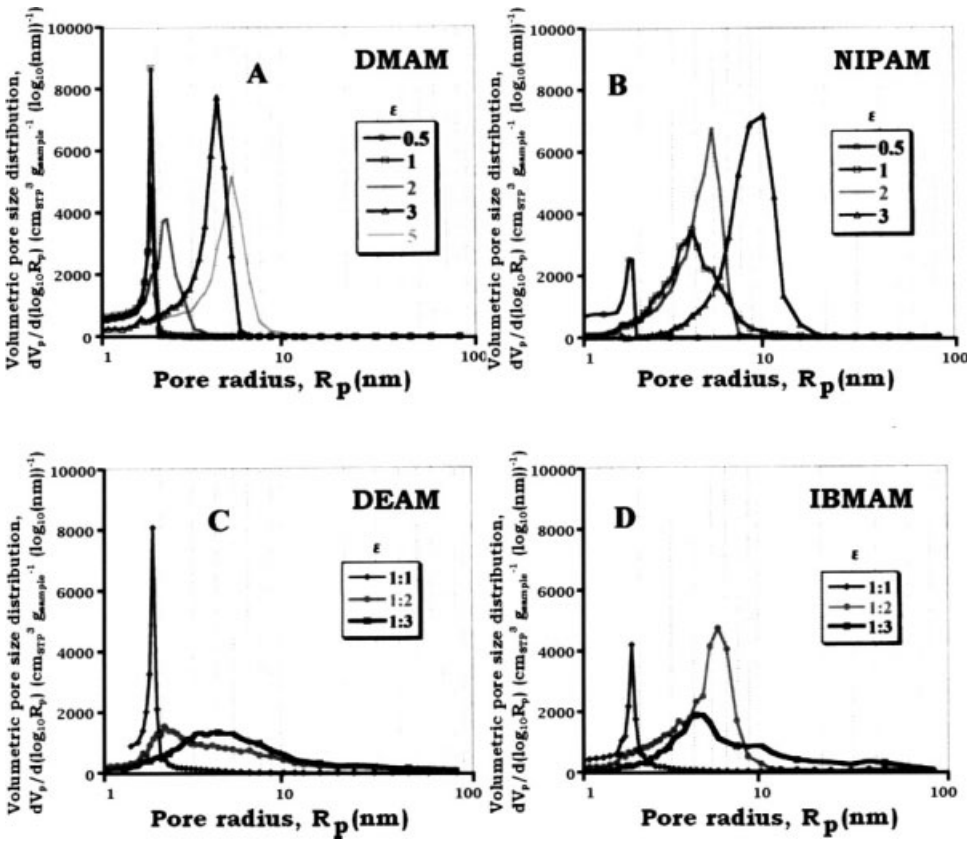

Figure 5 Volumetric pore size distributions evaluated from the nitrogen desorption profiles at 77 K. (A) DMAM, (B) NIPAM, (C) DEAM, and (D) IBMAM. The weight ratios ε of the template hydrogel to the silica matrix are shown in the figures.

In addition, the total volume of the nanopore noticeably decreased when the template hydrogel was changed from NIPAM to DEAM. (Note that the total volume of the nanopore can be compared by seeing the area below the pore size distribution profiles in Figure 5.) The result indicates that the proportion of the template hydrogel moiety, which completely separated out of the silica matrix and did not contribute to the formation of the nanopores, increased as the template hydrogel became more nonpolar.

Figure 6 presents the values of the standard deviation of the radius of the nanopores evaluated with respect to the pore volume V_p. First, the standard deviation increased as the template hydrogel became less polar. Second, the degree of the increase in the standard deviation enhanced in the same shift in the polarity as shown earlier. Third, the above enhancement most stood out between the two cases of NIPAM and DEAM. Basically, the increase in the standard deviation means the broadening of the pore size distribution. That is, a part of the template hydrogel segregated from the silica matrix to form the pores, which were too large to be captured by the nitrogen adsorption. Therefore, the trend of the increasing pore size with the nonpolarity of the template hydrogel well coincided with the illustrations derived from the other experimental results.

CONCLUSIONS

To clarify the effect of the polarity of the hydrogel species on the replicated nanoporous structure into the silica matrix, we used the following four

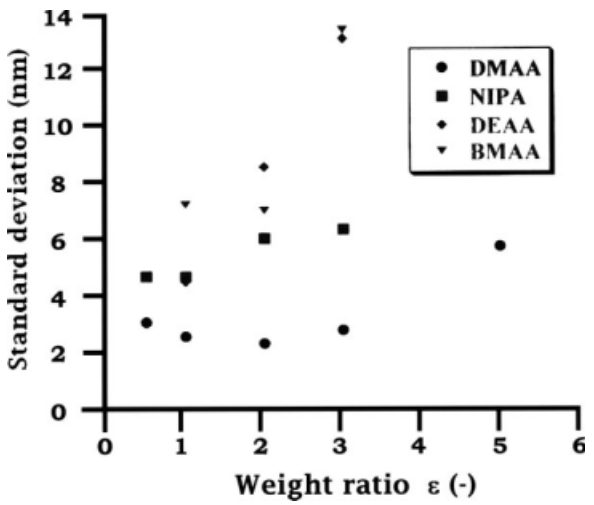

Figure 6 Dependence of the standard deviation of the radius of the nanopores on the weight ratio ε. The standard deviations were evaluated with respect to the volume of the nanopores. The legend symbols corresponding to the respective hydrogel species are shown in the figure.

hydrogels with the polarity varied by the hydrophobic end groups (Fig. 1), DMAM, NIPAM, DEAM, and IBMAM. The size of the nanopores in the silica replica of hydrogel increased with the decrease in the polarity of the hydrogel. Furthermore, the distribution of the pore size broadened in parallel. The hydrogel with the larger polarity had less tendency of segregating from the hydrogel template swollen with water.

The authors gratefully acknowledge Mr. N. Takane and H. Kanbara. They are also thankful to Dr. K. Susa for many enlightening discussion throughout this work.

References

1. Tan, C.; Lu, R.; Xue, P.; Bao, C.; Zhao, Y. Mater Chem Phys 2008, 112, 500.
2. Lopez-Ureta, L. C.; Orozco-Guareño, E.; Cruz-Barba, L. E.; Gonzalez-Alvarez, A.; Bautista-Rico, F. J Polym Sci Part A: Polym Chem 2008, 46, 2667.
3. Fu, X. J.; Wang, N. X.; Zhang, S. Z.; Wang, H.; Yang, Y. J. J Inorg Mater 2008, 23, 393.
4. Ford, J.; Yang, S. Chem Mater 2007, 19, 5570.
5. Nelson, K.; Deng, Y. Macromol Mater Eng 2007, 292, 1158.
6. Zhao, J.; Li, Y.; Cheng, G. Chin Sci Bull 2007, 52, 1796.
7. Shen, Z.; Duan, H.; Frey, H. Adv Mater 2007, 19, 349.
8. Sahiner, N. Colloid Polym Sci 2006, 285, 283.
9. Bao, C.; Lu, R.; Xue, P.; Jin, M.; Tan, C.; Liu, G.; Zhao, Y. J Nanosci Nanotechnol 2006, 6, 807.
10. Zhao, J.; Li, Y.; Kuang, Q.; Cheng, G. Colloid Polym Sci 2005, 284, 175.
11. Firestone, M. A.; Dietz, M. L.; Seifen, S.; Trasobares, S.; Miller, D. J.; Zaluzec, N. J. Small 2005, 1, 754.
12. Marty, J. D.; Mauzac, M. Adv Polym Sci 2005, 172, 1.
13. Aburto, J.; Mendez-Orozco, A.; Le Borgne, S. Chem Eng Process 2004, 43, 1587.
14. Bao, C.; Lu, R.; Jin, M.; Xue, P.; Tan, C.; Zhao, Y.; Liu, G. J Nanosci Nanotechnol 2004, 4, 1045.
15. Jung, J. H.; Lee, S. S.; Shinkai, S.; Iwaura, R.; Shimizu, T. Bull Korean Chem Soc 2004, 25, 63.
16. Wang, H.; Holmberg, B. A.; Yan, Y. J Am Chem Soc 2003, 125, 9928.
17. Shen, X.; Tong, H.; Jiang, T.; Zhu, Z.; Wan, P.; Hu, J. Compos Sci Technol 2007, 67, 2238.
18. Matsusaki, M.; Yoshida, H.; Akashi, M. Biomaterials 2007, 28, 2729.
19. Hutchens, S. A.; Benson, R. S.; Evans, B. R.; O'neill, H. M.; Rawn, C. J. Biomaterials 2006, 27, 4661.
20. Sugawara, A.; Yamane, S.; Akiyoshi, K. Macromol Rapid Commun 2006, 27, 441.
21. Hawkins, D. M.; Stevenson, D.; Reddy, S. M. Anal Chim Acta 2005, 542, 61.
22. Alexandre, E.; Cinqualbre, J.; Jaeck, D.; Richert, L.; Isel, F.; Lutz, P. J. Macromol Symp 2004, 210, 475.
23. Bellamkonda, R.; Ranieri, J. P.; Bouche, N.; Aebischer, P. J Biomed Mater Res 1995, 29, 663.
24. Kurumada, K.; Nakamura, T.; Suzuki, A.; Umeda, N.; Kishimoto, N.; Hiro, M. J Non-Cryst Solids 2007, 353, 4839.
25. Kurumada, K.; Nakamura, T.; Suzuki, A.; Umeda, N. Adv Powder Technol 2007, 18, 763.
26. Kurumada, K.; Suzuki, A.; Otsuka, E.; Basa, S.; Seto, Y.; Morita, K.; Nakamura, T. Prog Colloid Polym Sci 2009, 136.
27. Barrett, E. P.; Joyner, L. J.; Halenda, P. P. J Am Chem Soc 1951, 73, 373.